Journal of Thermal Analysis and Calorimetry, Vol. 59 (2000) 143–155

Dedicated to Prof. Edith A. Turi in recognition of her leadership in education

THERMAL AND DYNAMIC-MECHANICAL CHARACTERIZATION OF UNI- AND BIAXIALLY ORIENTED POLYPROPYLENE FILMS

M. B. Elias[1], *R. Machado*[2] *and S. V. Canevarolo*[1]*

[1]Materials Engineering Department, Universidade Federal de São Carlos
[2]Centro de Caracterização e Desenvolvimento de Materiais, Universidade Federal de São Carlos SP, Brazil

Abstract

The effect of uni- and biaxial orientation in the morphology of polypropylene films has been investigated by thermal, dynamic-mechanical, X-ray pole figure and diffraction patterns. In uniaxial oriented films the level of damping is roughly three times higher in the MD direction than it is in the TD direction. The stretching always produces crystals of the α form independently of the starting type. Fast DSC scans show two melting peaks indicative of two crystalline species. The Fujiyama *et al.* model for the crystalline structure can be also applied to the uniaxially stretched films. Upon biaxially orienting, the folded lamellae crystals (kebabs) are the ones to support all the force applied, and when their maximum level of stress slippage is reached they deform following the Peterlin's model, forming a new shish structure. These new shishes are aligned to the TD direction and by linking the original shishes in the MD direction produce a planar orthogonal net of linked shish structures. The space among the shishes is filled with small and imperfect folded lamellae with *c*-axis in the film plane and preferentially oriented in the MD and TD directions, keeping constant crystallinity density throughout.

Keywords: biaxially oriented PP, damping, morphology model, uniaxially oriented polypropylene, β-PP

Introduction

Isotactic polypropylene is a versatile olefinic thermoplastic with great commercial importance, with applications ranging from moulded articles, fibres, films, etc. Its semi-crystalline structure is formed mainly by a monoclinic lattice called α form with well defined crystal parameters [1]. The crystalline morphology obtained during cooling from the melt, in the absence of flow, is the characteristic spherulitic structure. In this arrangement a pile of folded chain lamellae, nucleated inside the molten polymer, grows radially filling the whole space with alternating layers of lamella surrounded by amorphous phase. To maintain a constant density the average distance between two adjacent lamellae must be kept constant and so taking into account that

* Author for correspondence: e-mail: caneva@power.ufscar.br

1418–2874/2000/ $ 5.00
© 2000 Akadémiai Kiadó, Budapest
Akadémiai Kiadó, Budapest
Kluwer Academic Publishers, Dordrecht

the growth is radial the lamella ought to branch several times. A second crystal type found in PP shows a hexagonal lattice called β form [2] which also forms spherulitic structures.

Through DSC curves it is possible to verify the polymorph nature of the polypropylene. The α form is the more stable and show a melting temperature in the range of 165 °C and the less stable β form melts at lower temperatures. Upon stretching the β form can be converted in the α form [3–4]. The crystalline molecular orientation can be evaluated by analysing the X-ray diffraction patterns presented in a form of pole figures. From there one can get information about the crystalline orientation distribution, i.e. the crystalline texture. The most important diffraction planes of the polypropylene in the α form are: (110) at 2θ≅16.4°, (040) at 2θ ≅19.7°, (130) at 2θ ≅ 21.6° and in the β form are: (300) at 2θ ≅17.8° and (301) at 2θ ≅22.7°, using cobalt radiation [5].

Various authors have studied fibres and uniaxially oriented films being the work of Samuels [6] one of the most important work. Even though biaxially oriented films are quite important commercially, few researchers have worked with it, pointing out Okajima *et al.* [7–10], de Vries *et al.* [11–12] and Ward *et al.* [13]. Recent studies on biaxially oriented films in the presence of β nucleating agents were realised by Kimura *et al.* [14–15] and of blends with hydrogenated oligocyclopentadiene by Barczak *et al.* [16].

Peterlin [17] has proposed a model for the changes in morphology during cold drawing of a folded chain lamellar morphology. During deformation the spherulites initially spherical are elongated and soon loose any recognisable shape. The lamellae slide and reorient themselves in the direction of stretching piling into microfibrils with a great number of intercrystalline links.

Shish-kebab structures [18–19] tend to appear when flow is present during the solidifying amorphous phase. This structure is formed by a fibrilar core consisting of mainly elongated chains called shish, in which spaced in a regular manner, a folded chain lamella crystallises and grows sideways called kebab. Experimentally the flow of the chains have been imposed initially mainly by Couette stirring [20]. Adding to the great crystal orientation its anisotropy one should expected sizeable variations in the thermal and mechanical properties associated with the macroscopic orientation of a sample containing oriented shish-kebab structures.

Fujiyama *et al.* [21] using the shish-kebab morphology proposed a model of crystalline structure for the skin portion of injection moulded parts. The morphology is composed of shishkebab-like main skeleton structure, whose *c*-axis is parallel to the machine direction. The kebabs lamellar structures are linked by both, shish fibrous crystals and interlamellar chains. Piled epitaxially on the *c*-axis-oriented lamellae are small, imperfect and non uniform lamellae whose a^*-axes are oriented with the MD direction.

The present work deals with the characterization of the crystalline morphology during biaxially orientation of polypropylene films. For this purpose we closely follow its effects in thermal and dynamic-mechanical behaviour and X-ray scattering of unstretched, uniaxially and biaxially stretched polypropylene films.

Experimental

Materials and methods

The polymer matrixes used in this work are all extrusion grade PP homopolymer: a standard type (OPP Petroquimica S.A., Brazil, MI=3 g/10 min, density ρ=0.9 g cm^{-3}), a high crystallinity grade HCPP (with higher isotacticity) and a β nucleated (NJSTAR supplied by New Chemical Co. Ltd. Kyoto).

Film extrusion and stretching

The films were extruded in a Brückner industrial biaxially orienting machine at VOTOCEL Filmes Flexíveis Ltda (Brazil). The extrudate as a molten flat sheet is cooled and crystallised in a water bath, than heated up to approximately 110°C, stretched along to the extrusion direction, called machine direction MD, to a variable extent (in this work 3.5×, 4.5× and 5.5× the original length). Finally the temperature is increased to approximately 155°C and the film is stretched again in the transverse direction TD to a fixed total deformation of 10× the original width. For this work samples were cut at three different stages during the process: a) just after the water cooling bath, prior to the first stretch and called unstretched film, b) after the first stretching and called uniaxially stretched film and c) at the end of the process, called biaxially oriented film. Table 1 shows the dimensions of the standard PP film after each step of stretching.

Table 1 Film dimensions in each step of the stretching procedure (standard type)

	MD stretch ratio	TD stretch ratio	Width/m	Thickness/μm
Unstretched	–	–	0.71	750
Uniaxially stretched	3.5	–	0.63	245
	4.5	–	0.63	210
	5.5	–	0.6	190
Biaxially oriented	3.5	10	5.5	20
	4.5	10	5.5	18
	5.5	10	5.5	18

Thermal analysis

The dynamic-mechanical thermal analysis, using a calibrated [22] Rheometric Sci. DMTA IV equipment, was done in the tensile mode, at a frequency of 10 Hz and a heating rate of 3°C/min in films cut along MD and across TD the extrusion direction. The differential scanning calorimetry analysis, using a calibrated Perkin Elmer (DSC 7) equipment, was done in discs cut from the films and pilled in a number enough to get approximately 10 mg. To increase thermal contact and reduce sample

wobbling due to shrinkage during heating all pans with the sample were pressed in a manual wise to a constant compression deformation. The thermal curves were obtained during the first heating, from room temperature to 190°C, at various heating rates (5, 10 and 40°C min^{-1}).

Wide angle X-ray diffraction (WAXD)

WAXD pattern were obtained in a Siemens model D5000, operating at 40 kV, 40 mA, using radiation K_α from cobalt (Co) filtered with iron. Unstretched and uniaxially oriented films were measured as it is and biaxially oriented thin films were piled (≅25) and glued together with dried PVAl aqueous solution. The pole figures were obtained employing an Eulerian texture goniometer by tilting (scanning angle from $0 \leq \chi \leq 90°$) and rotating (scanning angle from $0 \leq \varphi \leq 360°$) the piled film samples, measuring every 5°, in reflection from $0 \leq \chi \leq 50°$ and transmission from $50 \leq \chi \leq 90°$ modes [23–24]. Corrections for amorphous scattering, defocalisation and absorption effects were applied.

Results

Dynamic-mechanical thermal analysis (DMTA)

In order to evaluate the morphology of the biaxially oriented polypropylene films, we measured the tanδ and loss modulus E'' as a function of temperature, particularly in the range of the T_g of the PP matrix ($-40\,°C \leq T \leq 80\,°C$). The maximum intensity of the damping peak in a specific transition is directly proportional to the volume fraction of the transition phase [25]. On increasing the content of the amorphous phase, there is a linear increase in the maximum intensity of the damping peak and in its area. Figure 1a shows the tanδ damping curve of the three types of films used (standard, HCPP and β nucleated). The samples were obtained just after the water-cooling bath prior to the first stretch. The level of orientation at this stage is expected to be low but samples were cut to be tested along (MD) and across (TD) the machine direction. For each type of matrix the tanδ data in both cross directions are quite close confirm the lack of a preferential structural orientation at this early stages of the process. The β nucleated film shows the higher damping values indicating to be the less crystalline, and the HCPP shows the lower damping i.e. the higher crystalline sample in comparison with the standard PP. The loss modulus (Fig. 1b) keeps a fairly constant value in the range of 100 MPa independent of the sample orientation.

These same dynamic-mechanical parameters were also measured in the standard PP samples that have been uniaxially oriented stretched 3.5, 4.5 and 5.5 times its original length at 110°C, shown in Fig. 2. Due to the great orientation into the machine direction the two perpendicular directions do not show any longer the same level of damping being its value roughly three times as big as in the machine direction (max $\tan\delta \cong 0.095 \pm 0.005$) than it is in the transverse direction (max $\tan\delta \cong 0.035 \pm 0.005$). The loss modulus (Fig. 2b) follows closely the same behaviour showing one order of magnitude in difference be-

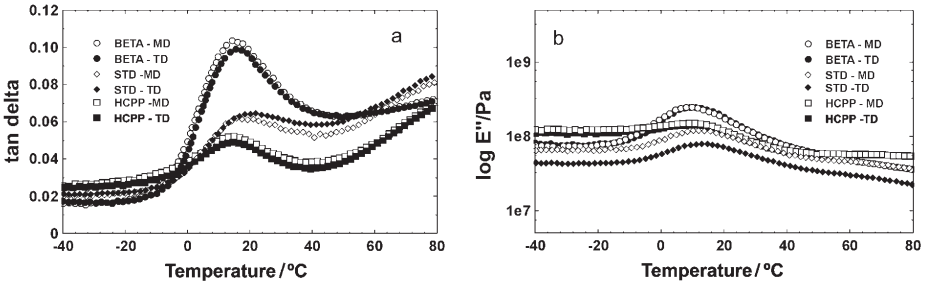

Fig. 1 Tensile tanδ (a) and loss modulus (b) curves of the non-oriented films used (standard, HCPP and β nucleated) in the range of the T_g of the PP matrix

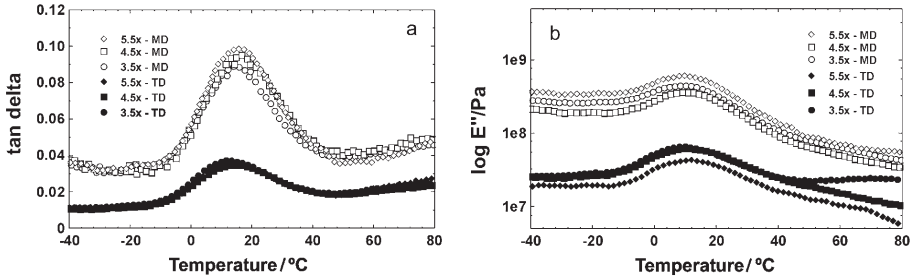

Fig. 2 Tensile tanδ (a) and loss modulus (b) curves of the uniaxially oriented standard PP films in the range of the T_g of the PP matrix, stretched 3.5, 4.5 and 5.5×

tween the two perpendicular directions (50 MPa for the TD and 500 MPa for the MD directions). The different levels of orientation used show minor changes in the tanδ and E'' values.

A comparison in the tanδ behaviour among all three types of PP, uniaxially oriented and stretched 5.5× is shown in Fig. 3. The differences in tanδ behaviour seen in the two figures before are still present: a) samples with higher crystallinity (HCPP) shows lower damping values and b) the MD direction shows higher damping (Fig. 3a) and loss modulus (Fig. 3b) than the TD direction. The explanation for the first effect was already given during the discussion of Fig. 1 and the second will be discussed later in this work.

Upon biaxially orienting the various PP matrixes the difference in the behaviour of damping is systematically reduced with the increase in the levels of stretching, tending to a common value of damping at the peak, i.e. max tanδ≅0.04±0.01, when the maximum practical stretch level is reached (5.5×10). This convergence of damping behaviour with increasing levels of stretch can be seen in the Fig. 4 for the biaxially oriented films. Curves of loss modulus are somehow more scattered but show that the peak value of the MD direction has dropped from 500 to 100 MPa, with a considerable increase in the transverse TD direction from 50 to 400 MPa.

Differential scanning calorimetry (DSC)

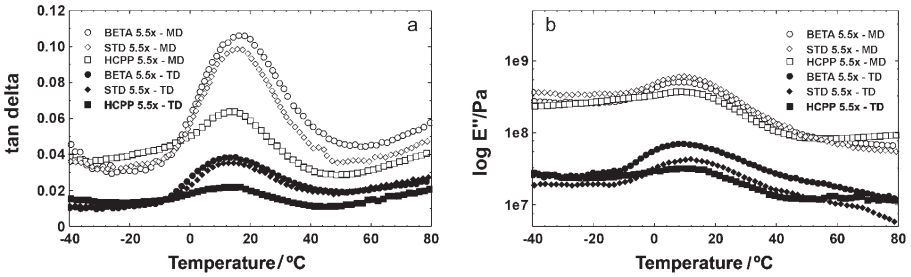

Fig. 3 Tensile tanδ (a) and loss modulus (b) curves of the uniaxially oriented samples (standard, HCPP and β nucleated) films in the range of the T_g of the PP matrix, stretched 5.5×

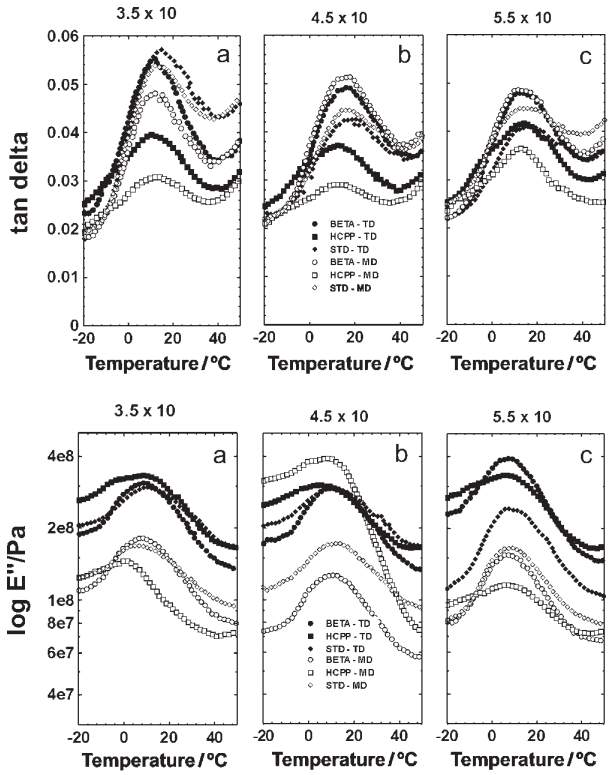

Fig. 4 Tensile tanδ and loss modulus curves of the biaxially oriented PP films in the range of the T_g of the PP matrix, with various level of stretching a) 3.5×10, b) 4.5×10 and c) 5.5×10

Figure 5 shows the DSC curves of unstretched, uniaxially (5.5×) and biaxially (5.5×10) oriented standard PP films, measured at 40°C min^{-1}. The fast heating rate was employed to reduce recrystallization during the melting scan. The unstretched sample obtained just after the water cooling bath prior to the first stretch presents a spherulitic crystallization type structure without any appreciably level of orientation: its fusion behaviour denotes typically this crystalline morphology with only one and broad melting peak with T_m=164°C. The uniaxially oriented film shows two melting peaks one at 162°C and another higher up at 170°C. The biaxially oriented film also shows two peaks one at 163°C and another at 174°C. Smaller shoulders are also present. If smaller heating rate is employed the same two peaks behaviour is obtained (not shown) for the uni- and biaxially oriented films.

The high crystallinity polypropylene HCPP shows in broad sense the same results (Fig. 6) as the standard PP but the peak values are displaced a few degrees higher. The high isotacticity permits the formation of thicker lamellae, which shows higher melting temperature. Again, if smaller heating rate is employed, the same two peaks behaviour is obtained (not shown) for the uni- and biaxially oriented films.

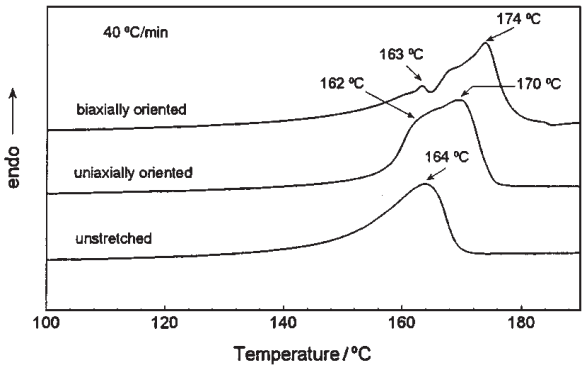

Fig. 5 DSC melting curves of unstretched, uniaxially (5.5) and biaxially (5.5×10) oriented standard PP films (40°C min^{-1})

The β nucleated polypropylene unstretched film is composed mainly of a β spherulitic structure which melts in the range of 140–150°C. A pure β form sample is difficult to obtain there always being present a certain amount of α form (this fact will be corroborated later using WAXD diffraction patterns). During the heating the melted β crystals immediately recrystallize into the more stable α form which in its turn melts at 164°C. This phenomenon is seen as two melting peaks and to avoid misinterpretation (e.g. with the two melting peaks of two different crystalline species) usually different heating rates are employed and compared, as shown in Fig. 7. The scan at 5°C min^{-1} presents a much higher concentration of high melting temperature species (α form melting at 164°C) than the curve obtained at 40°C min^{-1}. The low heating rate allows that the kinetics of melting the β phase and its recrystallization in α form happens.

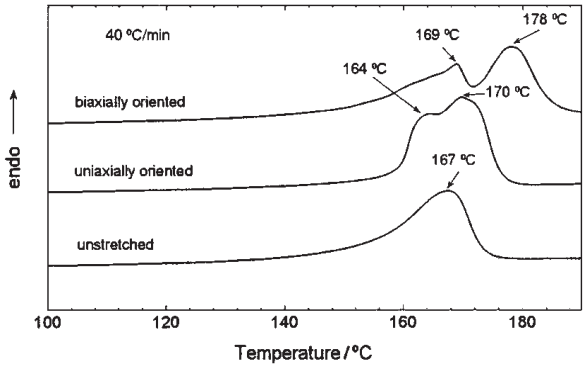

Fig. 6 DSC melting curves of unstretched, uniaxially (5.5) and biaxially (5.5×10) oriented high crystallinity HCPP films (40°C min^{-1})

Figure 8 shows the DSC curves of unstretched, uniaxially (5.5×) and biaxially (5.5×10) oriented originally β nucleated PP films, measured at a fast heating rate (40 °C min^{-1}). The curve of the unstretched sample was already shown and discussed in the previous figure (it is shown again here for the sake of comparison). Upon stretching, the original spherulitic structure is destroyed and converted into an oriented shish-kebab structure that melts above 164°C. Again the uniaxially oriented film shows two melting peaks at 168°C and 172°C. The biaxially oriented film also shows two peaks at 163°C and 174°C. Smaller shoulders are also present.

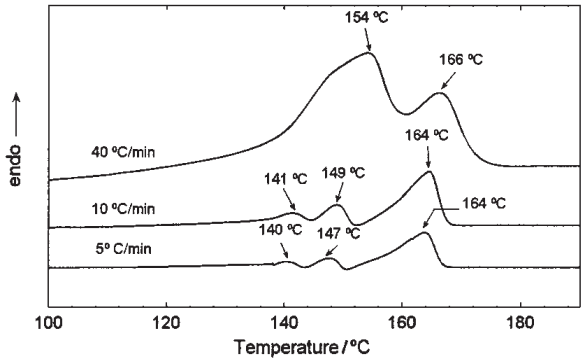

Fig. 7 DSC melting curves of unstretched β nucleated polypropylene films scanned at 5, 10 and 40 °C min^{-1}

To confirm and identify the two crystalline species detected by DSC a WAXD pattern of the unstretched, uniaxially and biaxially oriented β nucleated films were obtained and are shown in Fig. 9. The unstretched β nucleated polypropylene film (Fig. 9a) shows a strong peak at 2θ=18.7°, due to the plane (300) of the β form, overlapped by weak peaks of the α form. On the other hand uni- and biaxially oriented

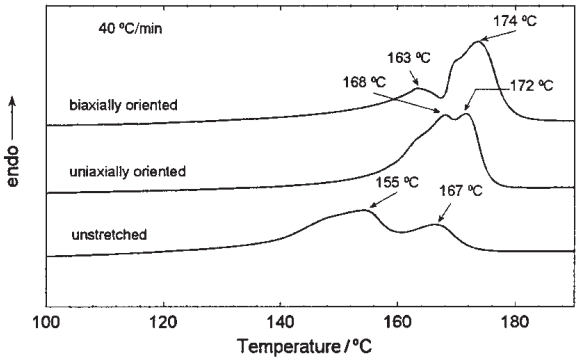

Fig. 8 DSC melting curves of β nucleated of unstretched, uniaxially (5.5) and biaxially (5.5×10) oriented films (40 °C min^{-1})

samples (Figs 9b and 9c respectively) consist of only α form crystals, with same crystalline texture. Standard and HCPP samples show in all cases only α form.

The crystalline orientation in the films can be evaluated by X-ray pole figures, as shown in Fig. 10. We choose the (110) diffraction planes (2θ≅16.4°) as the more convenient one because the (040) plane (2θ≈19.7°) gives a too intense and the (130) (2θ≈21.6°) a rather weak signal to allow an even equilibrium among the three signals. Following its diffraction intensity by rotating the film around the two axes (χ and φ) we can have a good idea of the orientation distribution intensities in the sample. Unstretched films have a spherulitic crystalline structure, not having any macroscopic preferential orientation direction and so its (110) diffraction intensity is low and evenly distributed in all three directions (machine direction MD, transverse direction TD and normal direction ND) in the film (Fig. 10a). After uniaxial stretching

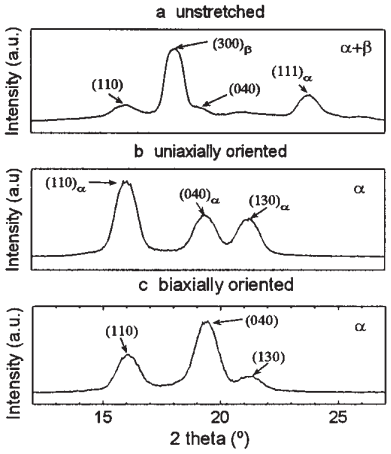

Fig. 9 WAXD pattern of the a) unstretched, b) uniaxially and c) biaxially oriented β nucleated PP films

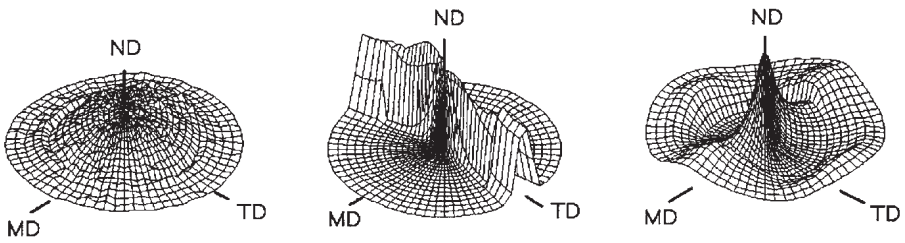

Fig. 10 X-ray pole figures of (110) diffraction plane: a) unstretched, b) uniaxially (5.5) and c) biaxially (5.5×10) oriented standard PP films. MD: machine direction, TD: transverse direction and ND: normal direction

the pole figure shows a characteristic fan-like shape aligned with the TD direction indicating that the '*c*' axis is aligned preferentially in the machine direction (Fig. 10b). With the biaxial stretching, as shown in the Fig. 10c, the fan-like shape is reduced to five symmetrical peaks: one intense at the centre characteristic of the (110) planes and four others at χ=72° and φ=0, 90, 180 and 270°, confirming that the (040) diffraction planes are also parallel to the film plane (the angle between (110) and (040) planes is 72°). These intensities are strong and even distributed in both stretching directions (MD has φ=0 and 180° and TD has φ=90 and 270°), presenting also a weak halo.

Discussion

The tanδ damping and loss modulus data for the unstretched sample are quite close in both cross directions confirming that there is no preferential molecular or crystalline orientation. The DSC curve shows a characteristic pattern of a spherulitic crystalline structure with broad lamellae thickness distribution.

Upon uniaxial orientation the level of damping changes quite dramatically being its value in the MD direction roughly three times as big as in the TD direction. Samples with higher crystallinity (HCPP) shows lower damping values due to the low amorphous phase content. The loss modulus is one scale of magnitude higher in the MD direction. The stretching produces always crystals of the α form independently of the starting type. Fast DSC scans for β nucleated PP films show two melting peaks, indicative of two crystalline species.

We think that, up to this moment, the model proposed by Fujiyama *et al.* [21] for the skin portion of injection moulded parts could be applied for the uniaxially stretched films without any alteration. The morphology consists of shish-kebab-like main skeleton structure, whose *c*-axis is parallel to the machine direction. The kebabs lamellar structures are linked by both, shish fibrous crystals and interlamellar chains. Piled epitaxially on the *c*-axis-oriented lamellae are small, imperfect and non uniform lamellae whose *a**-axis are oriented with the MD direction. During the stretching the original spherulitic structure is destroyed and converted, via Peterlin's model into an

oriented shish-kebab structure. It shows two melting peaks at different temperature, due to the two types of crystal, folded lamellae or kebabs and extended fibrils or shish. X-ray pole figure shows a fan-like shape pattern indicating that the main *c*-axis of the crystals (either lamellae or fibrils) are oriented mainly with the MD direction but without any preferential orientation in its orthogonal plane. If we consider the great crystal orientation and its inherent anisotropy one should expect considerable anisotropy in the thermal and mechanical properties of the uniaxially oriented films. The presence of kebabs linked only to one shish produce an anisotropic structure, which greatly increases the damping in the MD direction.

After biaxial orientation the difference in behaviour of the damping is systematically reduced with the increase in the levels of the MD stretching, tending to a common value when the maximum practical stretch level is reached. Due to machine design and construction we have to take into account that the level of stretching in the transverse direction TD is constant and fixed in 10 times (10×). The convergence of data leads to a balanced thermal and mechanical behaviour in both perpendicular directions when the increasing in the levels of stretch in the MD direction reaches the maximum in practical terms. DSC curves still show two crystalline species: lamella and fibrous crystals melting at different temperatures. Smaller shoulders are also present and can be attributed to badly form crystal structures, probably during the secondary crystallization, after the biaxial stretching. The X-ray pole figure is converted into five symmetrical peaks in the film plane, due to the (110) and (040) diffraction planes.

Following the results shown so far we can, starting from the model of Fujiyama *et al.*, extend it to suit the morphological rearrangements, which happens during the biaxial stretch. During the TD deformation the folded lamellae crystals (kebabs) are the ones to support all the stress applied, not affecting the shish structures, placed in the perpendicular direction. Reaching a minimum level of stress slippage the folded lamellae deforms following the Peterlin's model, forming a new shish structure. Lamellae that are linked to two shishes are the ones more likely to extend. The new shishes formed are aligned to the TD direction and links the original shishes producing, in a larger scale, a planar orthogonal net of linked shish structures. Figure 11 shows a diagram of the proposed crystalline structure. The orthogonal shish net can be seen as symmetrical peaks at 72°, mainly aligned into both direction (MD and TD). To keep constant density distribution throughout, the space among the shishes is filled with small and imperfect folded lamellar structures, with *c*-axis oriented preferentially in the MD and TD directions, in the film plane (weak halo at χ=72°).

Conclusions

Thermal, mechanical and X-ray measurements have allowed us to conclude that the model of Fujiyama *et al.* for the crystalline structure of a skin layer in injection-moulded PP can be also applied to the uniaxially stretched films. Extending this model further we propose that the crystalline structure of a biaxially oriented film be

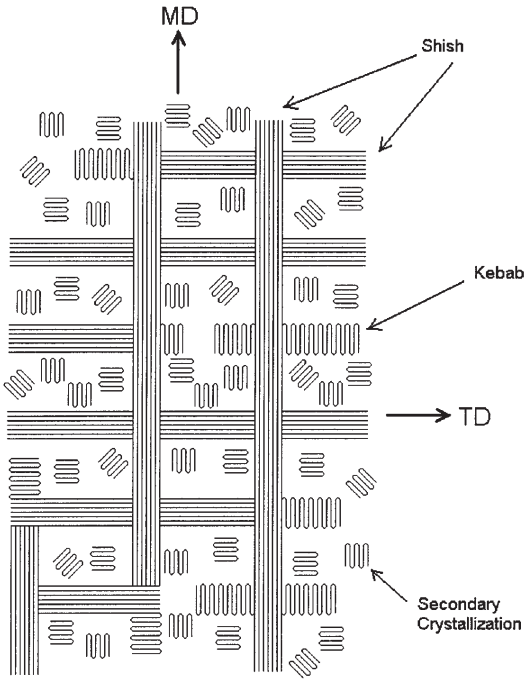

Fig. 11 Proposed structural model for the biaxially oriented polypropylene film

made of a planar orthogonal net of linked shish structures. The space among the shishes is filled with small and imperfect folded lamellar structures with *c*-axis in the film plane and preferentially oriented in the MD and TD directions, keeping a constant crystallinity density throughout.

* * *

The authors wish to thank CNPq (PRONEX), CAPES, FINEP and FAPESP for funding various projects and Marcelo B. Elias particularly acknowledges CAPES for his financial support. We also thank VOTOCEL for kindly providing the oriented films and support the publication of the results.

References

1 G. Natta and P. Corradini, Nuovo Cimento, Suppl., 15 (1960) 40.
2 H. D. Keith, F. J. Padden Jr., N. M. Walker and H. W. Wyckoff, J. Appl. Phys., 30 (1959) 1485.
3 V. Vittoria, 'Handbook of Polymer Science and Technology', v. 2, Performance Properties of Plastics and Elastomers, Marcel Dekker Inc., New York 1989 p. 507–556.
4 J. Varga, in 'Polypropylene – Structure, Blends and Morphology', J. Karger-Kocsis, (ed), v. 1, Chapman and Hall Ltd., Cambridge 1995, p. 56–115.
5 Z. W. Wilchinsky, J. Appl. Phys., 31 (1960) 1969–1972.

6 R. J. Samuels, 'Structured Polymer Properties – The Identification, Interpretation and Application of Crystalline Polymer Structure', John Wiley & Sons Inc., New York 1974.
7 H. Tanaka, T. Masuko and S. Okajima, J. Appl. Polym. Sci., 17 (1973) 1715.
8 N. Iwato, H. Tanaka and S. Okajima, J. Appl. Polym. Sci., 17 (1973) 2533.
9 N. Iwato, H. Tanaka and S. Okajima, J. Appl. Polym. Sci., 19 (1975) 303.
10 H. Tanaka and S. Okajima, Polym. Letters Edit., 15 (1977) 349.
11 A. J. De Vries, Pure & Appl. Chem., 53 (1981) 1011.
12 A. J. De Vries, Pure & Appl. Chem., 54 (1982) 647.
13 I. Karacan, A. K. Taraya, D. I. Bower and I. M. Ward, Polymer, 34/13 (1993) 2691.
14 C. Feng, T. Yamaoka, H. Ide and Y. Kimura, Polymer, 35/16 (1994) 3442.
15 F. Chu and Y. Kimura, Polymer, 37/4 (1996) 573.
16 E. Martuscelli and Z. Bartczaj, Polymer, 38/16 (1997) 4139.
17 A. Peterlin, J. Appl. Phys., 48/10 (1977) 4099.
18 A. J. Pennings and A. M. Kiel, Kolloid-Z, 205 (1965) 160.
19 A. Keller and M. J. Machin, J. Macromolec. Sci.-Phys., B2, (1968) 501.
20 A. J. Pennings, A. A. Van der Mark and A. M. Kiel, Kolloid-Z, 237 (1970) 336.
21 M. Fujiyama, T. Wakino and Y. Kawasaki, J. Polym. Sci., 35 (1988) 29.
22 C. Lotti and S. V. Canevarolo, Polym. Test, 17 (1998) 523.
23 L. E. Alexander, X-ray Diffraction Methods in Polymer Science, John Wiley & Sons Inc., New York 1969 p. 209–240.
24 M. Kakudo and N. Kasai, X-Ray Diffraction by Polymers, Kodansha Ltd., Tokyo, 1972 p. 231–270.
25 R. E. Wetton, Develop. Polym. Charact., Chap. 5, Appl. Sci. Publ. (1986).